Journal of RADIATION INDUSTRY

Vol. 19, No. 2, pp. 173-183, 2025
https://doi.org/10.23042/radin.2025.19.2.173

Original article

Comprehensive Photoprotective Effects of Centipedegrass (*Eremochloa ophiuroides*) Extract Against Ultraviolet-Induced Skin Damage

Seong Hee Kang[1,†], Hanui Lee[2,†], Mi Yeon Kim[2], Chang Won Kang[1], and Seung Sik Lee[2,3,*]

[1]Technology Research Institute of Biomaysin, Jeongeup, Jeollabuk-do 56212, Republic of Korea
[2]Radiation Biotechnology Division, Advanced Radiation Technology Institute (ARTI), Korea Atomic Energy Research Institute (KAERI), Jeongeup, Jeollabuk-do 56212, Republic of Korea
[3]Department of Radiation Life Science, University of Science and Technology (UST), Daejeon 34113, Republic of Korea

ABSTRACT Centipedegrass (*Eremochloa ophiuroides*) extract is rich in flavonoid compounds such as maysin, isoorientin, orientin, luteolin, and their glycosylated derivatives. These compounds exhibit strong UV-A absorption capacity, with maximum absorbance (λmax) typically observed in the 340-350 nm range. While their direct UV-B absorption is limited due to the absence of λmax within the 280-320 nm range, the extract demonstrates significant potential in alleviating UV-B-induced cellular damage through its potent antioxidant activity. In this study, we investigate the photoprotective effects of CGE, focusing on its UV-A absorbance properties and reactive oxygen species (ROS) scavenging ability. The results suggest that the synergistic combination of UV-A filtering and antioxidative protection positions CGE as a promising natural agent for broad-spectrum photoprotection.

Key words: Centipedegrass, Antioxidant, UV protection, Sunscreen

1. Introduction

Ultraviolet (UV) radiation constitutes approximately 5% of solar energy reaching the Earth's surface and is divided into UV-C (100-280 nm), UV-B (280-320 nm), and UV-A (320-400 nm) based on wavelength [1]. While UV-C is largely filtered by the ozone layer, UV-B and UV-A reach the skin and exert a range of biological effects [2]. UV-B radiation penetrates the epidermis, where it causes direct DNA damage, inflammatory responses, erythema, and is strongly associated with photocarcinogenesis [3]. In contrast, UV-A radiation penetrates deeper into the dermis, inducing reactive oxygen species (ROS) generation, leading to long-term effects such as photoaging, collagen degradation, and loss of skin elasticity [4]. Therefore, developing effective agents for UV protection has long been a critical area of research in the functional cosmetics industry.

Conventional UV protection strategies typically rely on inorganic UV filters (e.g., titanium dioxide, zinc oxide) or organic chemical absorbers (e.g., oxybenzone, avobenzone) [5]. However, several synthetic UV filters have raised concerns due to potential adverse effects such as skin irritation, allergic reactions, phototoxicity, and endocrine disruption [6]. As a result, the demand for natural, skin-friendly, and eco-conscious photoprotective agents has been steadily growing. Among them, plant-derived flavonoids are gaining attention as dual-function agents with both UV absorption capabilities and potent antioxidant activities.

Flavonoids are a class of polyphenolic compounds based on the benzopyran core structure and are classified into flavones, flavonols, flavanones, and anthocyanins, among others [7]. Flavones, in particular, exhibit notable UV absorption properties. C-glycosylated flavones at the 6- or 8- position show increased water solubility and reduced skin irritation, making them favorable for topical applications [8]. Their UV absorbance is primarily attributed to the conjugated π-electron systems across the A and B rings, enabling $\pi \rightarrow \pi^*$ transitions [9,10]. UV absorption typically occurs in two regions: Band I (320-380 nm, B-ring cinnamoyl system) and Band II (250-280 nm, A-ring benzoyl system) [11,12].

Centipedegrass (*Eremochloa ophiuroides*) is a C4 warm-season grass previously considered a weed or turfgrass [13]. Recent

ISSN 1976-2402 **http://www.ksri.kr/**

Copyright© 2025 by Korean Society of Radiation Industry

[†]These authors contributed equally to this work.

***Corresponding author:** Seung Sik Lee
Tel: +82-63-570-3332, Fax: +82-63-570-3339, E-mail: sslee@kaeri.re.kr

Received 9 June 2025 **Revised** 18 June 2025 **Accepted** 18 June 2025

phytochemical studies have identified this species as a novel source of bioactive flavonoids such as maysin (6-C-glucosyl-O-rhamnosyl apigenin), isoorientin, orientin, luteolin, rhamnosylisoorientin, derhamnosylmaysin, and eremonetin [14,15]. These compounds, predominantly C-glycosylated flavones, display strong UV-A absorption with λmax values around 340-350 nm, which correspond to the Band I region.

Despite the absence of absorption peaks in the UV-B range (280-320 nm), these compounds exhibit robust antioxidant activities, enabling them to mitigate UV-B-induced cellular oxidative stress indirectly. Numerous studies have demonstrated that such flavonoids suppress ROS generation, lipid peroxidation, and the expression of matrix metalloproteinases (MMPs), thus providing photoprotection through non-absorptive mechanisms [16-18]. These biological activities are attributed to their electron-donating properties and metal ion-chelating capacities [19].

This study aims to evaluate the UV absorption profile and antioxidant potential of CGE to assess its viability as a natural photoprotective ingredient. We focus on demonstrating the dual-function mechanism of the extract: direct UV-A absorption and indirect protection against UV-B-induced oxidative stress, thereby proposing CGE as a promising candidate for multifunctional, plant-based sun care applications.

2. Materials and Methods

2.1. Preparation of CGE

CGE was prepared following a previously reported method with modifications [20].Briefly, seeds of CGE were obtained from Fukukaen Nursery (Blu Co. Ltd.) and cultivated at the Korea Atomic Energy Research Institute (KAERI) in 2016. The harvested leaves were stored at −80°C until use. Dried centipedegrass leaves (5 kg) were pulverized using a Wiley mill (Indian Weiber) and sieved through a 420 μm mesh.

For hot water extraction, 250 g of dried leaves were extracted with 5 L of distilled water at 90°C for 6 h. The extract was filtered twice through Whatman filter papers (No. 2, Ø110 mm), followed by a third filtration using a 0.45 μm syringe filter to remove fine particulates. The resulting filtrates were concentrated under reduced pressure and stored at −20°C until further analysis.

2.2. Determination of Total Phenolic Content (TPC)

The total phenolic content (TPC) of CGE was quantified using the Folin-Ciocalteu colorimetric method. Briefly, the extract was mixed with Folin-Ciocalteu's phenol reagent and incubated for 1 h at room temperature in the dark. After the reaction, 200 μL of each sample was transferred into wells of a 96-well microplate, and absorbance was measured at 765 nm using a microplate reader (Tecan, Männedorf, Switzerland). For quantification, a calibration curve was generated using gallic acid as a standard, and results were expressed as milligrams of gallic acid equivalents per gram of dried extract (mg GAE/g). Each sample was measured in triplicate, and results are presented as the mean ± standard deviation (SD).

2.3. Determination of Total Flavonoid Content (TFC)

The total flavonoid content (TFC) of CGE was determined using a colorimetric assay based on aluminum nitrate complexation. Briefly, 500 μL of the extract solution (prepared by mixing the extract with methanol at a 1:9 ratio, w/v) was mixed with 100 μL of 10% aluminum nitrate [$Al(NO_3)_3$] and 100 μL of 1 M potassium acetate (CH_3COOK). Subsequently, 4.3 mL of methanol was added to the mixture, followed by incubation at room temperature for 40 minutes. After the reaction, absorbance was measured at 415 nm using a UV-Vis spectrophotometer. Quercetin was used as the reference standard, and the total flavonoid content was calculated based on a quercetin calibration curve prepared using the same procedure. Results were expressed as milligrams of quercetin equivalents per gram of dried extract (mg QE/g). All measurements were performed in triplicate and presented as mean ± standard deviation (SD).

2.4. DPPH radical scavenging assay

The DPPH (2,2-diphenyl-1-picrylhydrazyl) radical scavenging activity of CGE was measured following a modified version of Blois' method [21]. Briefly, 500 μL of sample solution at various concentrations (10-1,000 μg/mL) was mixed with 500 μL of 300 μM DPPH solution in ethanol. The mixture was incubated in the dark at 37°C for 30 minutes. After incubation, 200 μL of the reaction mixture was transferred into a 96-well plate, and absorbance was measured at 517 nm using a microplate reader (Tecan, Männedorf, Switzerland). (+)-catechin (100 μg/mL) was used as the positive control. The radical scavenging activity was calculated using the following formula:

$$\text{Scavenging activity (\%)} = \left[1 - \frac{A_{sample} - A_{blank}}{A_{control}}\right] \times 100$$

2.5. ABTS radical cation decolorization assay

ABTS radical scavenging activity was determined using the method of Re *et al*. [22]., with slight modifications. $ABTS^{\bullet+}$ was generated by reacting 7 mM ABTS solution with 2.45 mM potassium persulfate, followed by incubation in the dark for 12-16 h. The $ABTS^{\bullet+}$ solution was diluted with ethanol to obtain an absorbance of 0.70±0.02 at 734 nm. For the assay, 100 μL of the extract solution was mixed with 900 μL of the diluted $ABTS^{\bullet+}$ solution, and after 10 min of incubation at room temperature, absorbance was measured at 734 nm using a microplate reader (Tecan, Männedorf, Switzerland).

2.6. Measurement of UV Absorbance of Centipedegrass extract (CGE)

CGE was serially diluted to final concentrations of 10, 5, 2.5, 1, 0.5, and 0.1 mg/mL using appropriate solvents. Subsequently, 100 μL of each diluted sample was loaded into wells of a 96-well black microplate. UV absorbance spectra were measured at 5 nm intervals over the range of 230-400 nm using a microplate reader (Tecan, Männedorf, Switzerland).

2.7. HPLC analysis

CGE were analyzed to identify maysin and its derivatives by using an Agilent Technologies 1200 series HPLC apparatus (Agilent Technologies Inc., Santa Clara, CA). Separation was performed using a YMC-Pack ODS A-302 column (4.6 mm i.d.×150 mm; YMC Co., Ltd., Kyoto, Japan) as described by Lee *et al*. [14] at a flow rate of 1 mL/min. The mobile phase consisted of 1% formic acid (solution A) and 100% methanol (solution B), and the elution was performed by a combined step and linear gradient from 100:0 (solutions A: B) to 50:50 in 30 min, followed by 50:50-0:100 in 60 min. The eluted compounds were detected at a wavelength of 360 nm, and a sample volume of 20 μL was injected.

2.8. Cell culture

Human dermal fibroblasts (CCD-986SK) were purchased from the Korean Cell Line Bank (KCLB, Seoul, Korea). Cells were cultured in Iscove's Modified Dulbecco's Medium (IMDM; Gibco, USA) supplemented with 10% fetal bovine serum (FBS), 100 U/mL penicillin, and 100 μg/mL streptomycin. The fibroblasts were maintained in a humidified incubator at 37°C with 5% CO_2 atmosphere, and subcultured at 70-80% confluence for subsequent experiments.

2.9. Evaluation of UVB-Induced Cytotoxicity Using MTT Assay

To evaluate the cytotoxic effects of UVB radiation on dermal fibroblasts, CCD-986SK cells were seeded at a density of 1×10^4 cells/well in 96-well plates and cultured for 6 hours in complete medium containing 10% fetal bovine serum (FBS). The medium was then replaced with serum-free medium, and cells were incubated overnight. Subsequently, cells were exposed to UVB radiation at various doses (1, 5, 10, 15, 20, 25, and 30 mJ/cm^2) using a calibrated UVB lamp. After irradiation, cells were incubated for an additional 24 hours at 37°C in serum-free medium. Following the incubation, the culture medium was removed and cells were washed once with phosphate-buffered saline (PBS). Then, 100 μL of fresh medium containing 100 μg/mL of MTT [3-(4,5-dimethylthiazol-2-yl)-2,5-diphenyltetrazolium bromide] was added to each well and incubated for 3 hours at 37°C. After incubation, cells were washed again with PBS and the resulting formazan crystals were dissolved in 100 μL of dimethyl sulfoxide (DMSO). Absorbance was measured at 540 nm using a microplate reader (Infinite M200, Tecan, Männedorf, Switzerland). Cell viability was expressed as a percentage of the control group (non-irradiated cells).

2.10. Measurement of intracellular oxidative stress

CCD-986SK human dermal fibroblasts were seeded at a density of 1×10^5 cells/well in 6-well plates and incubated with CGE (100 μg/mL) for 24 h at 37°C in a humidified 5% CO_2 atmosphere. Following incubation, the cells were exposed to UVB radiation at a dose of 30 mJ/cm^2. Intracellular oxidative stress was quantitatively assessed using the Muse™ Oxidative Stress Kit and Muse™ Cell Analyzer (EMD Millipore, Billerica, MA, USA) in accordance with the manufacturer's instructions. Briefly, cells were detached using trypsin-EDTA, centrifuged, and resuspended in assay buffer to a final concentration of 1×10^6 cells/mL. An equal volume of Muse™ Oxidative Stress working solution was added, and the mixture was incubated at 37°C for 30 minutes in the dark. Oxidized cells were then quantified by flow cytometric analysis based on red fluorescence intensity. The data were collected from four independent experiments and analyzed using Muse™ analysis software.

2.11. Protective effects of CGE against UVB-induced apoptosis in human dermal fibroblasts

To evaluate the photoprotective effects of CGE against

UVB-induced cell death, CCD-986SK human dermal fibroblasts were seeded at a density of 1×10^6 cells/well in 6-well plates and cultured overnight in complete medium (IMDM supplemented with 10% FBS) at 37°C in a humidified 5% CO_2 atmosphere. After incubation, the culture medium was removed, and cells were washed once with phosphate-buffered saline (PBS). Each well was then replenished with 1 mL of PBS. In parallel, 1 mL of either distilled water (DW) or CGE solution was placed in a separate 6-well plate. The two 6-well plates (cell-containing and extract-containing) were aligned and stacked such that the CGE or DW solution was positioned directly above the cells, without direct contact. Cells were then irradiated with UVB at a dose of 30 mJ/cm^2. After irradiation, the treatment plate was removed, and cells were incubated in serum-free medium for 24 hours under standard culture conditions (37°C, 5% CO_2). Following incubation, the medium was discarded, and the cells were washed with PBS and detached using 500 µL of trypsin. Cells were collected by centrifugation at 3,000 rpm for 3 minutes. The resulting cell pellets were stained using the Muse™ Annexin V & Dead Cell Assay Kit (MCH100105, EMD Millipore, Billerica, MA, USA), according to the manufacturer's instructions. Apoptotic and dead cell populations were quantified using a Muse™ Cell Analyzer (version 1.1.2; EMD Millipore, Billerica, MA, USA). All experiments were performed in triplicate.

3. Results

3.1. Total phenolic and flavonoid content of CGE

The total phenolic and flavonoid contents of CGE were quantitatively evaluated and compared to green tea extract as a reference standard. As shown in Fig. 1A, the total phenolic content of CGE was approximately 124.5±3.8 mg GAE/g, which was significantly higher ($p<0.001$) than that of green tea extract (68.7±4.2 mg GAE/g). Similarly, the total flavonoid content (Fig. 1B) was found to be 132.4±5.1 mg CE/g for CGE, again significantly exceeding the content in green tea extract (52.3±2.9 mg CE/g) with high statistical significance ($p<0.001$).

These findings demonstrate that CGE possesses a significantly higher concentration of phenolic and flavonoid compounds, many of which are recognized for their antioxidant and anti-photoaging activities. The higher bioactive content compared to green tea, a well-established antioxidant plant source, suggests that CGE may serve as a superior botanical candidate for functional applications in skin protection and health supplements.

3.2. Antioxidant activity of CGE

The antioxidant potential of CGE was evaluated using both DPPH and ABTS radical scavenging assays across concentrations ranging from 10 to 1000 µg/mL. (+)-Catechin served as the positive control in both assays. In the DPPH assay (Fig. 1C), CGE exhibited a concentration-dependent increase in free radical scavenging activity, starting at 18.33±2.17% (10 µg/mL) and reaching 103.15±3.18% at 1000 µg/mL, surpassing (+)-catechin (102.11±5.92%). The half-maximal inhibitory concentration (IC_{50}) was determined to be 81.54 µg/mL, indicating strong hydrogen-donating capacity. In the ABTS assay (Fig. 1D), CGE similarly demonstrated potent antioxidant activity. Scavenging efficiency increased from 25.00±1.60% at 10 µg/mL to 102.52±2.30% at 1000 µg/mL, approximating the activity of (+)-catechin (103.75±5.20%). The calculated IC_{50} for ABTS was 72.48 µg/mL, suggesting higher aqueous-phase antioxidant efficacy. These findings collectively confirm the strong radical-scavenging potential of CGE.

3.3. UV–Vis Absorbance Spectrum of CGE

To evaluate the UV absorbance properties of CGE, UV-Vis spectra were recorded over the 240-400 nm range at varying concentrations (0.1 to 10 mg/mL). As shown in Fig. 2, the extract exhibited a concentration-dependent increase in absorbance intensity, particularly in the 340-350 nm region, where a distinct peak was observed. In contrast, no distinct λmax was observed within the UV-B region (280-320 nm), suggesting that the extract has limited direct UV-B absorption capability. Moderate absorbance was detected in the 250-280 nm range, consistent with Band II transitions (A-ring benzoyl system), but this falls outside the critical UV-B protection window. These results indicate that the CGE functions primarily as a UV-A shielding agent rather than a broad-spectrum UV filter.

3.4. HPLC-based quantification and UV-absorbance characterization of major bioactive compounds in CGE

High-performance liquid chromatography (HPLC) analysis was conducted to identify and quantify the major phytochemical constituents present in the CGE. The chromatogram (Fig. 3) revealed distinct peaks corresponding to known flavonoid and polyphenol compounds. Each compound was tentatively identified based on its retention time and spectral characteristics, and the quantitative contents were determined (Table 1). Among the identified compounds, derhamnosylmaysin was the most abundant (157.4±11.5 mg/g), followed by rhamnosylisoorientin (137.5±9.0 mg/g),

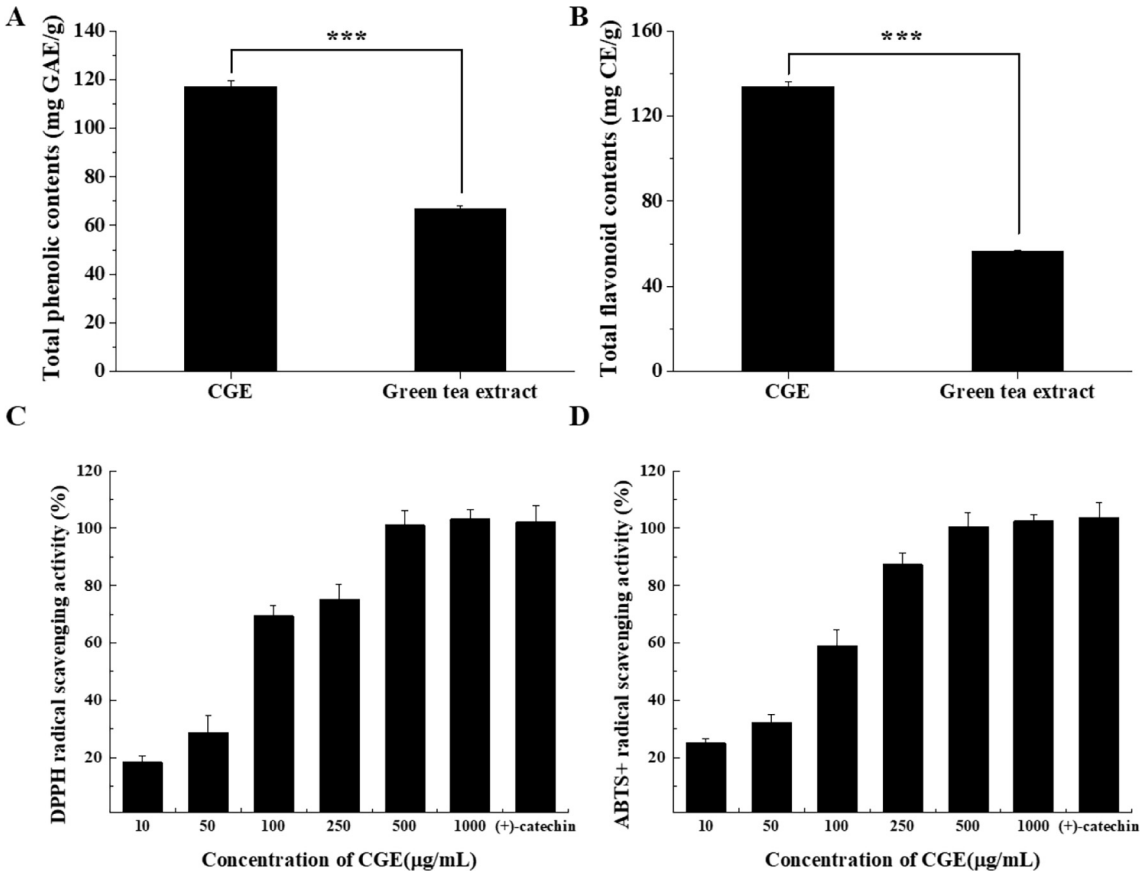

Fig. 1. Total phenolic and flavonoid contents and free radical scavenging activities of centipedegrass extract (CGE). The phenolic and flavonoid contents were measured by the Folin-Ciocalteu method and aluminum nitrate colorimetric assay, respectively. Antioxidant activities were assessed using DPPH and ABTS assays, showing dose-dependent scavenging effects comparable to (+)-catechin. Results are expressed as mean±SD from three independent experiments. **p<0.01, ***p<0.001 vs. green tea extract.

maysin (107.2±4.9 mg/g), and isoorientin (54.0±5.1 mg/g). Moderate concentrations of chlorogenic acid (67.6±3.7 mg/g), eremonetin (85.6±5.5 mg/g), luteolin (34.1±2.7 mg/g), and orientin (7.3±0.9 mg/g) were also detected.

The maximum UV absorbance wavelengths (λ_max) of the major components were predominantly located within the UV-A region (320-400 nm), indicating strong absorption characteristics. These UV absorption characteristics indicate that CGE is rich in C-glycosylated flavonoids with strong UV-A absorbance, particularly within the 345-351 nm range, corresponding to the Band I π→π* transition typical of flavone structures. The high levels of maysin derivatives and other polyphenols not only contribute to UV-A shielding but also suggest robust antioxidant potential, supporting the dual functionality of CGE as a natural photoprotective agent. Together, these results confirm that CGE harbors a unique composition of bioactive flavonoids capable of contributing to UV protection and oxidative stress mitigation, primarily through UV-A absorbance and antioxidant mechanisms.

3.5. Photoprotective and antioxidant effects of CGE against UVB-induced cytotoxicity

To investigate the photoprotective efficacy of CGE against UVB-induced cytotoxicity, a series of *in vitro* assays were performed using CCD-986SK human dermal fibroblasts. Initially, the cytocompatibility of CGE was confirmed by treating cells with various concentrations (0-1000 μg/mL) for 24 h and assessing viability via MTT assay. As shown in Fig. 4A, no significant differences in cell viability were observed at concentrations up to 200 μg/mL, indicating that CGE is well-tolerated by dermal fibroblasts within this range. Next, the sensitivity of fibroblasts to UVB irradiation was evaluated by exposing cells to increasing UVB doses (1-30 mJ/cm^2). A clear dose-dependent decline in cell viability was observed (Fig. 4B), with survival

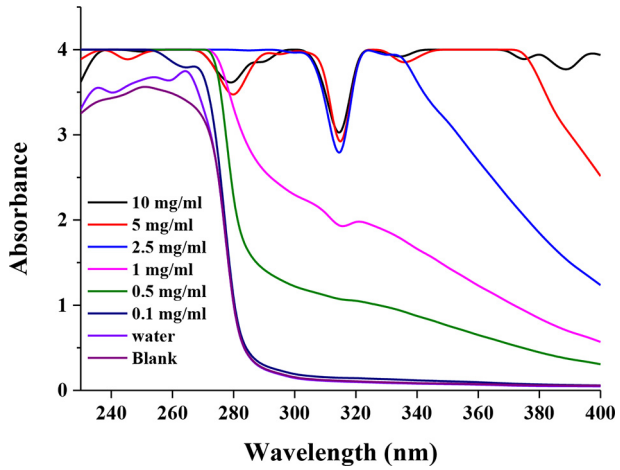

Fig. 2. UV-Vis absorption spectra of CGE at various concentrations. CGE was diluted to final concentrations of 0.1-10 mg/mL and scanned across the 230-400 nm range. UV absorbance was measured using a UV-Vis spectrophotometer. Water and blank served as controls.

Table 1. Quantification of Major Flavonoid and Phenolic Compounds in CGE. The concentrations of key bioactive compounds, including chlorogenic acid, orientin, isoorientin, rhamnosylisoorientin, derhamnosylmaysin, maysin, luteolin, and eremonetin, were determined in CGE using HPLC analysis. Results are expressed as milligrams per gram of dried extract (mg/g DW)

Compounds	Contents (mg/g)	λmax (nm)
Chlorogenic acid	67.6±3.7	325
Orientin	7.3±0.9	258, 351
Isoorientin	54.0±5.1	270, 350
Rhamnosylisoorientin	137.5±9.0	347
Derhamnosylmaysin	157.4±11.5	345
Maysin	107.2±4.9	346
Luteolin	34.1±2.7	345
Eremonetin	85.6±5.5	350

decreasing to approximately 25% at 30 mJ/cm^2, confirming the susceptibility of CCD-986SK cells to UVB-induced photodamage. To assess the intracellular oxidative stress generated by UVB and the potential antioxidant activity of CGE, intracellular reactive oxygen species (ROS) levels were measured using flow cytometry with a ROS-sensitive fluorescent probe. As illustrated in Fig. 4C, UVB exposure significantly elevated the proportion of ROS-positive cells (M2: 85.94%), compared to the control group (M2: 14.61%). Notably, co-treatment with CGE (1 mg/mL) during UVB exposure substantially reduced ROS-positive cells to 57.80%, indicating effective attenuation of oxidative stress by CGE. Quantitative analysis (Fig. 4D) confirmed this reduction to be statistically significant (***$p<0.001$). Furthermore, a dose-dependent protective effect of CGE against UVB was verified. Pre-treatment with CGE prior to UVB exposure (30 mJ/cm^2) restored cell viability in a concentration-dependent manner (Fig. 4E), with the 100 μg/mL treatment restoring viability to over 70% compared to 28% in the untreated UVB group (***$p<0.001$). These results demonstrate that CGE not only mitigates UVB-induced cytotoxicity but also suppresses intracellular oxidative stress, supporting its role as an effective antioxidant.

3.6. Interpretation and functional implications

Combined UV-Vis and HPLC analyses suggest that the photoprotective potential of CGE operates via a dual mechanism: I)

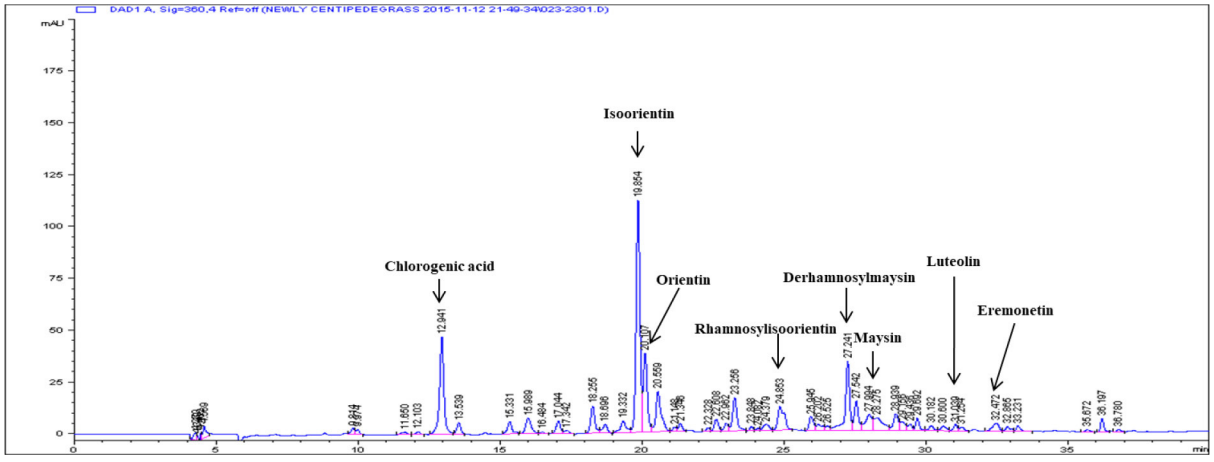

Fig. 3. Representative HPLC chromatogram of major flavonoids in CGE. Major flavonoid peaks were identified based on retention time and reference standards. Detection was carried out using a diode array detector (DAD) at 360 nm.

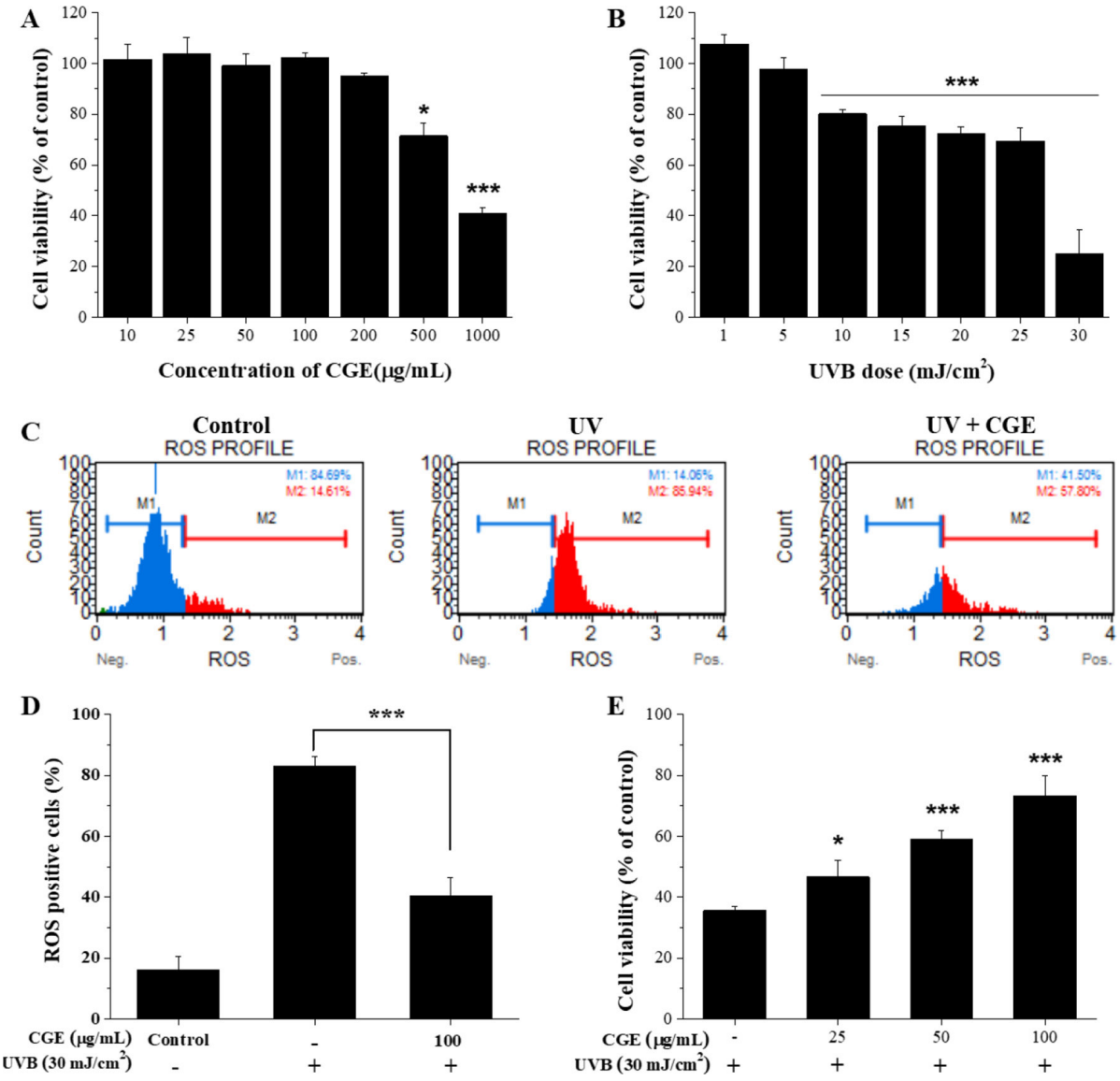

Fig. 4. Photoprotective and antioxidative effects of CGE on human dermal fibroblasts (CCD-986SK) under UVB irradiation. (A) Cell viability was assessed by MTT assay after treatment with increasing concentrations of CGE (25-100 μg/mL) for 24 h.(B) Dose-dependent cytotoxicity was analyzed following exposure to UVB radiation at doses ranging from 1-30 mJ/cm^2.(C) Intracellular ROS levels were measured by flow cytometry after UVB exposure (30 mJ/cm^2), with and without 100 μg/mL CGE overlay.(D) Quantification of ROS-positive cell populations from (C), indicating significant reduction of oxidative stress by CGE.(E) Protective effects of CGE against UVB-induced cytotoxicity at increasing concentrations, showing dose-dependent restoration of cell viability.Data are presented as mean±SD from three independent experiments. Statistical significance: ***p<0.001 vs. UVB only.

Direct UV-A absorption, attributable to high concentrations of flavonoids such as isoorientin, luteolin, and maysin derivatives, which exhibit strong absorbance in the 345-351 nm range (Band I). II) Indirect suppression of UVB-induced oxidative stress, through ROS-scavenging activity of phenolic compounds, notably maysin, derhamnosylmaysin, and rhamnosylisoorientin. Despite the absence of strong UVB absorbance in the UV spectrum, CGE demonstrated pronounced biological protection against UVB-induced cytotoxicity, likely mediated by intracellular antioxidant mechanisms. These findings affirm CGE's potential as a multifunctional photoprotective agent combining biochemical and photophysical attributes.

3.7. Protective effect of CGE as a physical UVB shield

To further evaluate the UVB-shielding capacity of CGE through physical means, a layer of 1 mg/mL CGE solution was

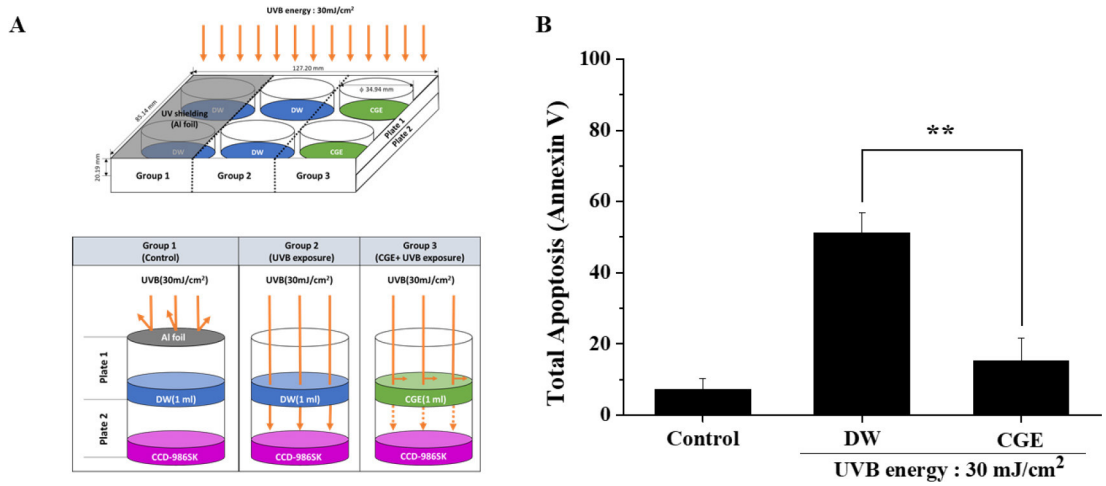

Fig. 5. Protective Effect of CGE as a Physical UVB Shield. (A) Schematic diagram of the *in vitro* experimental setup for evaluating the photoprotective effect of CGE against UVB radiation in CCD-986SK human dermal fibroblasts. Cells were divided into three groups: Group 1 (negative control, UVB-blocked with aluminum foil), Group 2 (UVB-exposed with distilled water), and Group 3 (UVB-exposed with CGE solution layered above cells). The extract was applied above the cell culture without direct contact to assess its physical UVB-blocking effect. (B) CCD-986SK cells were exposed to various intensities of UVB (1-30 mJ/cm^2), and cell viability was measured after 24 hours using the MTT assay. Data are expressed as percentage of control.

applied above fibroblast cultures during UVB irradiation (30 mJ/cm^2), simulating a topical barrier. This experimental design included: (1) a negative control group with UVB completely blocked by aluminum foil, (2) a UVB-only group with 1 mL distilled water overlay, and (3) a CGE-treated group with 1 mL of 1 mg/mL CGE overlay. As shown in Fig. 5, the UVB-only group (water overlay) displayed a markedly reduced cell viability of ~50%, while the CGE-overlay group demonstrated a significantly higher survival rate of ~85% ($p < 0.001$). The foil-shielded group showed negligible cytotoxicity, confirming effective UVB exclusion. These results indicate that CGE, even without direct cellular application, functions as a physical UVB barrier, possibly by absorbing, scattering, or attenuating incoming radiation. Together, these findings demonstrate that CGE exerts photoprotection via three distinct yet complementary mechanisms: (i) direct UV-A absorption by flavonoids, (ii) intracellular ROS neutralization, and (iii) physical attenuation of UVB penetration. These properties render CGE a strong candidate for incorporation into next-generation multifunctional photoprotective skincare formulations.

4. Discussion

In this study, we comprehensively evaluated the antioxidant activity and photoprotective capacity of CGE using a series of biochemical and cellular assays. The findings support the hypothesis that CGE provides dual-mode protection: through both direct absorption of UV radiation—particularly in the UVA spectrum—and indirect mitigation of UVB-induced oxidative stress via its rich content of polyphenols and flavonoids.

Antioxidant efficacy of CGE was demonstrated through DPPH and ABTS radical scavenging assays. Both assays revealed concentration-dependent scavenging activity, with CGE showing over 100% radical scavenging at 500-1000 μg/mL, comparable to (+)-catechin, a well-established positive control. Specifically, CGE exhibited 103.1% DPPH radical scavenging and 102.5% ABTS radical scavenging at 1000 μg/mL, highlighting its potent antioxidant potential. The relatively low standard deviations across concentrations also suggest experimental robustness. These outcomes are consistent with previous studies on plant-based polyphenols and support CGE's capacity to neutralize free radicals, a key mechanism in cellular protection against UV-mediated damage [23,24].

Supporting this antioxidant profile, the total phenolic and flavonoid contents of CGE were remarkably high (124.5 mg GAE/g and 132.4 mg CE/g, respectively), significantly surpassing those of green tea extract—a benchmark antioxidant botanical. These phytochemicals, including maysin, luteolin, isoorientin, and orientin, were identified via HPLC and are known for their ROS-scavenging, anti-inflammatory, and anti-aging effects [25].

The UV-Vis spectral analysis revealed that CGE exhibited strong absorbance in the UVA region (340-350 nm), with peak intensities corresponding to Band I π→π transitions commonly associated with flavone structures. Compounds such as isoorientin, orientin, and maysin—all C-glycosylated flavonoids—were identified as major UV-absorbing constituents with λ_max values ranging from 345 to 351 nm. In contrast, CGE showed relatively lower absorbance in the UVB range (280-320 nm), suggesting that its direct UVB-filtering capacity is limited compared to its pronounced UVA absorbance.

Interestingly, despite the lack of strong UVB absorption detected in the UV-Vis spectral analysis, CGE demonstrated a significant photoprotective effect against UVB-induced cytotoxicity *in vitro*. When used as a physical barrier (1 mg/mL overlay) during UVB irradiation, CGE markedly increased the viability of CCD-986SK human fibroblasts, restoring cell survival from approximately 30% (UVB only) to around 65% (UVB + CGE layer). This apparent discrepancy between the spectroscopic and biological results suggests that CGE can exert photoprotective effects through mechanisms other than direct molecular absorption of UVB photons. Several plausible explanations can be proposed:

First, scattering and reflection effects could play a substantial role [26]. The colloidal nature of the extract in aqueous media, combined with the optical density of polyphenolic constituents, may lead to partial scattering or deflection of UVB rays, thereby reducing the effective dose reaching the underlying cells [27,28]. Such particle-mediated optical effects are well-documented in plant-based formulations used for physical photoprotection [29,30].

Second, surface adsorption or partial absorption phenomena may contribute to UVB attenuation [31]. Even if CGE components do not exhibit strong peak absorbance within the 280-320 nm UVB range, cumulative weak absorbance across multiple wavelengths could collectively decrease UVB energy transmission [32]. Additionally, the hydrated film of CGE above the cell layer could act as a semi-absorptive medium, filtering UVB radiation indirectly.

In addition to passive shielding, the protective effect against UVB-induced apoptosis is likely attributed to CGE's bioactive compounds, which suppress intracellular ROS and downstream apoptotic signaling cascades. *In vitro* experiments using CCD-986SK human dermal fibroblasts demonstrated that CGE significantly mitigated UVB-induced cytotoxicity. Treatment with CGE prior to UVB exposure resulted in dose-dependent increases in cell viability, while flow cytometry showed a marked decrease in intracellular ROS accumulation. These findings support the hypothesis that CGE exerts its photoprotective effects in part by enhancing antioxidant defenses and buffering oxidative damage, possibly through activation of Nrf2/HO-1 pathways and suppression of pro-apoptotic signaling cascades such as JNK and caspase-3 [33].

Taken together, the dual mechanism—comprising UVA absorption by conjugated aromatic systems, UVB deflection, and antioxidant ROS neutralization—provides a synergistic photoprotective effect [34, 35].Such multifunctionality is highly desirable for next-generation plant-derived sunscreens, which seek to combine optical shielding with biological antioxidant protection without relying on synthetic chemical filters. Moreover, the observed effect underlines the importance of integrating both spectroscopic and cellular evaluations when assessing the photoprotective efficacy of botanical extracts. Future studies will be needed to quantitatively dissect the relative contributions of scattering, absorption, and antioxidant diffusion using more refined *in vitro* and ex vivo models. Additionally, *in vivo* studies will be crucial to validate the real-world efficacy and safety of CGE-based formulations under physiological conditions.

5. Conclusion

This study demonstrated that CGE possesses strong antioxidant and photoprotective properties, primarily attributable to its high content of polyphenolic compounds such as maysin, luteolin, isoorientin, and orientin. CGE showed potent free radical scavenging activity in both DPPH and ABTS assays, with IC_{50} values of 81.54 μg/mL and 72.48 μg/mL, respectively—comparable to those of established antioxidants. Although CGE exhibited limited direct UVB absorption in spectral analysis, its physical UVB-shielding effect and ROS-suppressing capacity significantly improved cell viability in UVB-exposed fibroblasts. These results suggest that CGE provides dual-mode photoprotection via UVA absorption and antioxidant defense against UVB-induced oxidative stress. Taken together, the findings of this study support the potential application of CGE as a multifunctional natural ingredient in the development of cosmeceuticals and photoprotective skincare formulations. Further *in vivo* studies and formulation evaluations will be instrumental in advancing CGE toward commercial utilization as a plant-derived UV protection agent.

Acknowledgments

This work was supported by Innopolis Foundation through Technology Commercialization Project, funded by Ministry of Science and ICT (Grant number. RS-2024-00416870).

References

1. Al-Sadek T, Yusuf N. 2024. Ultraviolet radiation biological and medical implications. *Curr Issues Mol Biol.* **46**(3):1924-42. https://doi.org/10.3390/cimb46030126.
2. D'Orazio J, Jarrett S, Amaro-Ortiz A, Scott T. 2013. UV radiation and the skin. *Int J Mol Sci.* **14**(6):12222-48. https://doi.org/10.3390/ijms140612222.
3. Mohania D, Chandel S, Kumar P, Verma V, Digvijay K, Tripathi D, Choudhury K, Mitten SK, Shah D. 2017. Ultraviolet radiations: Skin defense-damage mechanism. *Adv Exp Med Biol.* 71-87. https://doi.org/10.1007/978-3-319-56017-5_7.
4. Ciążyńska M, Olejniczak-Staruch I, Sobolewska-Sztychny D, Narbutt J, Skibińska M, Lesiak A. 2021. Ultraviolet radiation and chronic inflammation—Molecules and mechanisms involved in skin carcinogenesis: A narrative review. *Life (Basel).* **11**(4):326. https://doi.org/10.3390/life11040326.
5. Morabito K, Shapley N, Steeley K, Tripathi A. 2011. Review of sunscreen and the emergence of non-conventional absorbers and their applications in ultraviolet protection. *Int J Cosmet Sci.* **33**(5):385-90. https://doi.org/10.1111/j.1468-2494.2011.00654.x.
6. Wang J, Pan L, Wu S, Lu L, Xu Y, Zhu Y, Guo M, Zhuang S. 2016. Recent advances on endocrine disrupting effects of UV filters. *Int J Environ Res Public Health.* **13**(8):782. https://doi.org/10.3390/ijerph13080782.
7. Panche AN, Diwan AD, Chandra SR. 2016. Flavonoids: an overview. *J Nutr Sci.* **5**(e47). https://doi.org/10.1017/jns.2016.41.
8. Ali F, Rahul, Naz F, Jyoti S, Siddique YH. 2017. Health functionality of apigenin: A review. *International Journal of Food Properties.* **20**(6):1197-238. https://doi.org/10.1080/10942912.2016.1207188.
9. Gierschner J, Duroux J-L, Trouillas P. 2012. UV/Visible spectra of natural polyphenols: A time-dependent density functional theory study. *Food Chemistry.* **131**(1):79-89. https://doi.org/10.1016/j.foodchem.2011.08.034.
10. Di Meo F, Sancho Garcia JC, Dangles O, Trouillas P, 2012. Highlights on anthocyanin pigmentation and copigmentation: a matter of flavonoid π-stacking complexation to be described by DFT-D. *J Chem Theory Comput.* **8**(6):2034-43. https://doi.org/10.1021/ct300276p.
11. Sykuła A, Kowalska-Baron A, Gałęcki K, Błazińska P, Łodyga-Chruścińska. 2021. Structural and spectral investigation of a series of flavanone derivatives. *Molecules.* **26**(5):1298. https://doi.org/10.3390/molecules26051298.
12. Jung YS, Rha C-S, Baik M-Y, Baek N-I, Kim D-O. 2020. A brief history and spectroscopic analysis of soy isoflavones. *Food Science and Biotechnology.* **29**(1605-17). https://doi.org/10.1007/s10068-020-00815-6.
13. Li J, Guo H, Zong J, Chen J, Li D, Liu J. 2020. Genetic diversity in centipedegrass [Eremochloa ophiuroides (Munro) Hack.]. *Hortic Res.* **7**(4). https://doi.org/10.1038/s41438-019-0228-1.
14. Lee EM, Bai H-W, Lee SS, Hong SH, Cho J-Y, Lee I-C, Chung BY. 2012. Stress-induced increase in the amounts of maysin and maysin derivatives in world premium natural compounds from centipedegrass. *Radiation Physics and Chemistry.* **81**(8):1055-8. https://doi.org/10.1016/j.radphyschem.2012.01.002.
15. Lee EM, Lee SS, Bai H-W, Cho J-Y, Kim TH, Chung BY. 2013. Effect of gamma irradiation on the pigments and the biological activities of methanolic extracts from leaves of centipedegrass (Eremochloa ophiuroides Munro). *Radiation Physics and Chemistry.* **91**(108-13). https://doi.org/10.1016/j.radphyschem.2013.06.010.
16. Cos P, Calomme M, Sindambiwe J-B, De Bruyne T, Cimanga K, Pieters L, Vlietinck AJ, Berghe DV. 2001. Cytotoxicity and lipid peroxidation-inhibiting activity of flavonoids. *Planta Med.* **67**(06):515-9. https://doi.org/10.1055/s-2001-16472.
17. Slika H, Mansour H, Wehbe N, Nasser SA, Iratni R, Nasrallah G, Shaito A, Ghaddar T, Kobeissy F, Eid AH. 2022. Therapeutic potential of flavonoids in cancer: ROS-mediated mechanisms. **146**(112442). *Biomed Pharmacother.* https://doi.org/10.1016/j.biopha.2021.112442.
18. Lim H, Kim HP. 2007. Inhibition of mammalian collagenase, matrix metalloproteinase-1, by naturally-occurring flavonoids. *Planta Med.* **73**(12):1267-74. http://doi.org/10.1055/s-2007-990220.
19. Mucha P, Skoczyńska A, Małecka M, Hikisz P, Budzisz E. 2021. Overview of the antioxidant and anti-inflammatory activities of selected plant compounds and their metal ions complexes. *Molecules.* **26**(16):4886. https://doi.org/10.3390/molecules26164886.
20. Badaboina S, Bai H-W, Park C-H, Jang DM, Choi BY, Chung BYl. 2013. Molecular mechanism of apoptosis induction in skin cancer cells by the centipedegrass extract. *BMC Complement Altern Med.* **13**(350). https://doi.org/10.1186/1472-6882-13-350.
21. Blois MS. 1958. Antioxidant determinations by the use of a stable free radical. *Nature.* **181**(4617):1199-200. https://doi.org/10.1038/1811199a0.
22. Re R, Pellegrini N, Proteggente A, Pannala A, Yang M, Rice-Evans C. 1999. Antioxidant activity applying an improved ABTS radical cation decolorization assay. *Free Radic Biol Med.* **26**(9-10):1231-7. https://doi.org/10.1016/S0891-5849(98)00315-3.
23. Piazza S, Fumagalli M, Khalilpour S, Martinelli G, Magnavacca A, Dell'Agli M, Sangiovanni E. 2020. A review of the potential benefits of plants producing berries in skin disorders. **9**(6):542. *Antioxidants (Basel).* https://doi.org/10.3390/antiox9060542.
24. Hooda R, Madke B, Choudhary A. 2023. Photoaging: reversal of the oxidative stress through dietary changes and plant-based products. *Cureus.* **15**(4):e37321. http://doi.org/10.7759/cureus.37321.
25. Salehi B, Azzini E, Zucca P, Maria Varoni E, V. Anil Kumar N, Dini L. 2020. Plant-derived bioactives and oxidative stress-related disorders: a key trend towards healthy aging and longevity promotion. *Applied Sciences.* **10**(3):947. https://doi.org/10.3390/app10030947.
26. Julkunen-Tiitto R, Nenadis N, Neugart S, Robson M, Agati G, Vepsäläinen J. 2015. Assessing the response of plant flavonoids to UV radiation: an overview of appropriate techniques. *Phytochem Rev.* **14**(273-97). http://doi.org/10.1007/s11101-014-9362-4.
27. Oliveira H, Correia P, Pereira AR, Araújo P, Mateus N, de Freitas V, Oliveira J, Fernandes I. 2020. Exploring the applications of the photoprotective properties of anthocyanins in biological systems. **21**(20):7464. *Int J Mol Sci.* https://doi.org/10.3390/ijms21207464.
28. Salian A, Dutta S, Mandal S. 2021. A roadmap to UV-protective natural resources: Classification, characteristics, and applications. *Materials Chemistry Frontiers.* **5**(21):7696-723. https://doi.

org/10.1039/D1QM00741F.
29. Maurya SK, Divakar S, Patil UKJGJoP, Biomaterials. 2023. Potentials of plant derived products for the treatment of skin disorders. *German J Pharm Biomaterials.* **2**(3):9-31. https://doi.org/10.5530/gjpb.2023.3.8.
30. Nanda S, Madan K. 2021. The role of Safranal and saffron stigma extracts in oxidative stress, diseases and photoaging: A systematic review. *Heliyon.* **7**(2):e06117. http://doi.org/10.1016/j.heliyon.2021.e06117.
31. Li L, Chong L, Huang T, Ma Y, Li Y, Ding H. 2023. Natural products and extracts from plants as natural UV filters for sunscreens: A review. *Animal Model Exp Med.* **6**(3):183-95. https://doi.org/10.1002/ame2.12295.
32. Ferreyra MLF, Serra P, Casati P. 2021. Recent advances on the roles of flavonoids as plant protective molecules after UV and high light exposure. *Physiol Plant.* **173**(3):736-49. https://doi.org/10.1111/ppl.13543.
33. Khan NM, Ahmad I, Haqqi TM. 2018. Nrf2/ARE pathway attenuates oxidative and apoptotic response in human osteoarthritis chondrocytes by activating ERK1/2/ELK1-P70S6K-P90RSK signaling axis. *Free radical biology & medicine*. **116**(159-71). https://doi.org/10.1016/j.freeradbiomed.2018.01.013.
34. McDaniel D, Farris P, Valacchi G. 2018. Atmospheric skin aging—Contributors and inhibitors. *J Cosmet Dermatol.* **17**(2):124-37. https://doi.org/10.1111/jocd.12518.
35. Wondrak GT, Jacobson MK, Jacobson EL. 2006. Endogenous UVA-photosensitizers: mediators of skin photodamage and novel targets for skin photoprotection. *Photochem Photobiol Sci.* **5**(2):215-37. https://doi.org/10.1039/b504573h.